Penerbit Akademia Baru

Journal of Advanced Research in Fluid Mechanics and Thermal Sciences

Journal homepage: www.akademiabaru.com/arfmts.html
ISSN: 2289-7879

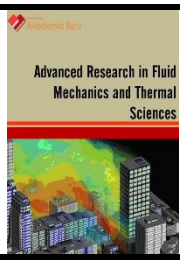

Developing Flow of Power-Law Fluids in Circular Tube Having Superhydrophobic Transverse Grooves

Open Access

Ming Wei Lee[1], Kok Hwa Yu[2,*], Yew Heng Teoh[2], Han Wei Lee[2], Mohd Azmi Ismail[2]

[1] School of Aerospace Engineering, Engineering Campus, Universiti Sains Malaysia, 14300 Penang, Malaysia
[2] School of Mechanical Engineering, Engineering Campus, Universiti Sains Malaysia, 14300 Penang, Malaysia

ARTICLE INFO

Article history:
Received 3 September 2018
Received in revised form 1 March 2019
Accepted 6 March 2019
Available online 7 March 2019

Keywords:
superhydrophobic, entrance length, water-repellent, surface roughness, laminar flow, non-Newtonian fluid

ABSTRACT

This study presents a numerical investigation on developing flow of inelastic non-Newtonian fluids in a circular tube having alternating superhydrophobic grooves and ribs arranged transversely to the flow direction. Laminar, steady and incompressible flow of non-Newtonian power-law fluid flowing in a circular tube having superhydrophobic transverse grooves of L = 0.1 and δ = 0.5 is considered. The influences arising from the presence of superhydrophobic surfaces (SHS) on radial velocity profile development, centerline velocity distribution and hydrodynamic entrance length are examined. For Reynolds numbers ranging from $Re = 1 \times 10^{-4}$ to $Re = 1$, numerical results show that the hydrodynamic entrance lengths arising from flow over superhydrophobic transverse grooves for non-Newtonian fluid with power-law index in the range $0.5 \leq n < 1.5$ are consistently longer than that of smooth surface.

1. Introduction

Superhydrophobic surface is widely used in many applications including lab-on-a-chip technology, thermal management, self-cleaning, condensation, etc. The prime benefit of superhydrophobic surface is its ability to reduce flow resistance and thus it is practically useful to gain higher mass flow rates through narrow channels when pumping power is limited [10,13,16]. This has been demonstrated in tubes with diameter in millimeters [17]. Most of recent studies on superhydrophobic surfaces are dedicated to fully-developed flow region [1,4,16,19], though there are a few exceptions [5,8,9,12,14,18,20]. At the entrance region, the flow would first experience a hydrodynamically developing flow region where viscous effect will give rise to redistribution of the flow and the development of boundary layers, before reaching a fully-developed flow condition where the velocity of the flow is no longer dependent on the axial direction. The length required to reach fully-developed flow region is known as hydrodynamic entrance length. In many microfluidics

* *Corresponding author.*
E-mail address: yukokhwa@usm.my (Kok Hwa Yu)

applications, developing flow region tends to prevail along the tube length, especially those having short tube lengths.

For Newtonian fluids flowing over smooth walls, the dimensionless hydrodynamic entrance length is found to vary nonlinearly with the Reynolds number [6]. In the presence of wall slippage, which can be modelled via enforcing uniform velocity slip length over the entire surface [5,8,12] or with surface having fully resolved superhydrophobic features [18,20], it gives rise to alteration on the entrance length and the velocity profile along the developing flow region. For Newtonian fluids flowing over superhydrophobic transverse grooves in channels [18] and tubes [20], the hydrodynamic entrance length is predicted to be longer than that of smooth walls. In other words, when superhydrophobic transverse grooves are employed along the walls, a greater length is required in order to achieve a hydrodynamically fully-developed flow condition. Instead of having Newtonian fluid, non-Newtonian fluid is often encountered in many chemical and processing industries. The non-Newtonian fluid behaviour could be modelled using the power-law fluid model with shear rate varies depending on the power-law index, i.e., $n < 1$ represents shear-thinning fluid and $n > 1$ represents shear-thickening fluid.

For a power-law fluid flowing in a circular tube of diameter D having smooth wall, the hydrodynamic entrance length can be approximated using correlation presented by Poole and Ridley [15], given by

$$\frac{L_h}{D} = [(0.246n^2 - 0.675n + 1.03)^{1.6} + (0.0567Re)^{1.6}]^{1/1.6} \quad (1)$$

where, L_h is the hydrodynamic entrance length and Re is the Reynolds number defined by [11,15]

$$Re = \frac{\rho {U_{avg}}^{2-n} D^n}{k} 8\left(\frac{n}{6n+2}\right)^n \quad (2)$$

where, U_{avg} is the average fluid velocity, ρ is the density of the fluid and k is the consistency index. It is worthwhile to note that the correlation stated in Eq. (1) is valid for power-law index ranging $0.4 < n < 1.5$ and Reynolds number in the range of $0 < Re < 1000$. A similar study has also been conducted recently for plane channel flow [7]. Both studies [7,15] show that the power-law index exhibits a significant influence on the hydrodynamic entrance length. In the absence of smooth surface, the influence of wall slip on hydrodynamic entrance length for non-Newtonian fluids has been recently studied, either employing wall slip [14] or with textured surfaces (i.e., superhydrophobic transverse grooves [9]). In the work documented by Haase *et al.,* [9], the hydrodynamic entrance length is predicted to be influenced by the gas fraction ratio and the normalized groove-rib periodic spacing. Apart from the effects arising from geometry of the textured surface, it will also be insightful to examine the influences of power-law index and Reynolds number on developing flow of power-law fluids in tube having superhydrophobic transverse grooves. It is worth to note that this paper focuses on Stokes flow ($Re \leq 1$) that typically arise in flow through narrow tubes having superhydrophobic surfaces [2,3,16].

2. Methodology

Consider a circular tube of diameter D in the cylindrical coordinate system (r, ϑ, z) with a periodic array of alternating superhydrophobic transverse grooves and ribs patterned along the tube wall, as shown in Figure 1. The axial and radial directions are represented by z and r directions, respectively. A groove-rib unit length is denoted by E and the width of the groove is e. The scale of the

superhydrophobic structures are governed by the dimensionless gas area fraction ($\delta = e/E$) and normalized groove-rib periodic spacing ($L = E/D$).

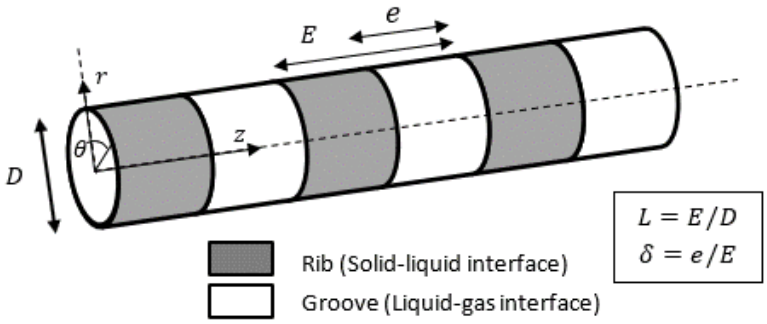

Fig. 1. Schematic diagram depicting flow in tubes having alternating superhydrophobic grooves and ribs

In this study, a steady laminar flow of incompressible power-law fluid passing through a circular tube without swirl ($u_\theta = 0$) is considered. The flow is axisymmetric about centerline and thus the flow field is independent of ϑ-direction. Based on the assumptions made, the governing mass and momentum conservation equations can be written as follows:

$$\frac{1}{r}\frac{\partial}{\partial r}(ru_r) + \frac{\partial u_z}{\partial z} = 0, \tag{3}$$

$$u_r\frac{\partial u_r}{\partial r} + u_z\frac{\partial u_r}{\partial z} = -\frac{1}{\rho}\frac{\partial p}{\partial r} + \frac{1}{r\rho}\frac{\partial(r\tau_{rr})}{\partial r} + \frac{1}{\rho}\frac{\partial \tau_{zr}}{\partial z} - \frac{\tau_{\theta\theta}}{r\rho}, \tag{4}$$

$$u_r\frac{\partial u_z}{\partial r} + u_z\frac{\partial u_z}{\partial z} = -\frac{1}{\rho}\frac{\partial p}{\partial z} + \frac{1}{\rho}\frac{\partial \tau_{zz}}{\partial z} + \frac{1}{r\rho}\frac{\partial(r\tau_{rz})}{\partial r} \tag{5}$$

where, τ_{rr}, τ_{zr}, $\tau_{\theta\theta}$, τ_{zz} and τ_{rz} are viscous stress components, given by

$$\tau_{rr} = \eta\left(2\frac{\partial u_r}{\partial r}\right) \tag{6}$$

$$\tau_{\theta\theta} = \eta\left(2\left(\frac{1}{r}\frac{\partial u_\theta}{\partial \theta} + \frac{u_r}{r}\right)\right) \tag{7}$$

$$\tau_{zz} = \eta\left(2\frac{\partial u_z}{\partial z}\right) \tag{8}$$

$$\tau_{rz} = \tau_{zr} = \eta\left(\frac{\partial u_r}{\partial z} + \frac{\partial u_z}{\partial r}\right) \tag{9}$$

The η denotes the power-law generalized Newtonian fluid (GNF) viscosity function, $\eta(\dot{\gamma}) = k\dot{\gamma}^{n-1}$ where k is the consistency index, $\dot{\gamma}$ is the rate of deformation and n is called the power-law index. For $n < 1$, the fluid exhibits shear thinning behaviour and $n > 1$ refers to fluid that shows shear thickening behaviour. Newtonian fluid is denoted by $n = 1$.

Governing equations in Eq. (3)-(5) are solved using ANSYS FLUENT 18.1, a finite volume based computational fluid dynamics (CFD) software package. The pressure-velocity coupling was solved via SIMPLE scheme. The numerical solution for pressure and momentum are based on second-order and second-order upwind schemes, respectively. To attain solutions with better accuracy, double

precision was used for all the calculations.The convergence ctiteria with scaled residuals of 10^{-10} for continuity and momentum equations are employed in this study. As illustrated in Figure 1, the solid-liquid (along ribs) and liquid-gas (along grooves) interfaces will give rise to two distinctly different values of shear stress. To mimic the effect of the mixed solid-liquid and liquid-gas interfaces, no-slip condition is imposed along the solid-liquid interface while shear-free condition is prescribed along the liquid-gas interface. It is also useful to highlight that there is no net mass flow rate through the gas layer, or in another word, the air on the superhydrophic surface is trapped. At the inlet ($z = 0$), a uniform velocity, U_{avg} is applied whereas a zero static pressure is precribed at the outlet.

3. Result and Discussion

In this numerical study, the diameter of the pipe (D) is 0.001m and the axial length (l) is 0.01m. The density and consistency index of the non-Newtonian fluid are prescribed to be 1000 *kg/m*^{3} and 1, respectively. The length of the pipe is sufficiently long to examine the entrance length for pressure-driven flow at low Reynold number ($Re \leq 1$). The Knudsen number of liquid is considered to be sufficiently low and thus rarefied effects are not considered. The hydrodynamic entrance length is defined when the centerline velocity reaches 99% of the fully-developed velocity (U_{FD}) in axial direction. The computational domain is confined in the domain of $(z, r) \in [0, l] \times [0, D/2]$. It is worth to mention that uniformly spaced structured grids are employed along axial and radial directions. To investigate the grid dependence of the numerical solution for pipe flow with transverse grooves, four grid resolutions are performed (i.e., $N_z \times N_r = 200 \times 10, 400 \times 20, 800 \times 40, 1600 \times 80$) for non-Newtonian fluids of $n = 0.5$ and $n = 1.5$. N_z and N_r are the number of elements in axial direction and radial direction, respectively. In this study, only superhydrophobic surface with transverse grooves of $L = 0.1$ and $\delta = 0.5$ is considered and the liquid-gas interface is assumed to be perfectly flat in the simulation. As can be seen from Figure 2, the solutions converge at higher grid resolutions. For $n = 1.5$, the dimensionless entrance length (L_h/D) is 0.5758 when grid resolution of $N_z \times N_r = 800 \times 40$ is employed. Doubling the grid resolution from 800 to 1600 elements for N_z and 40 to 80 elements for N_r results in only 0.49 % difference for (L_h/D). For $n = 0.5$, using the same set of grid resolutions, it would give rise to 0.18 % difference. To ascertain the accuracy of the results obtained via numerical simulation, grid resolution of $N_z \times N_r = 800 \times 40$ is best employed throughout this study.

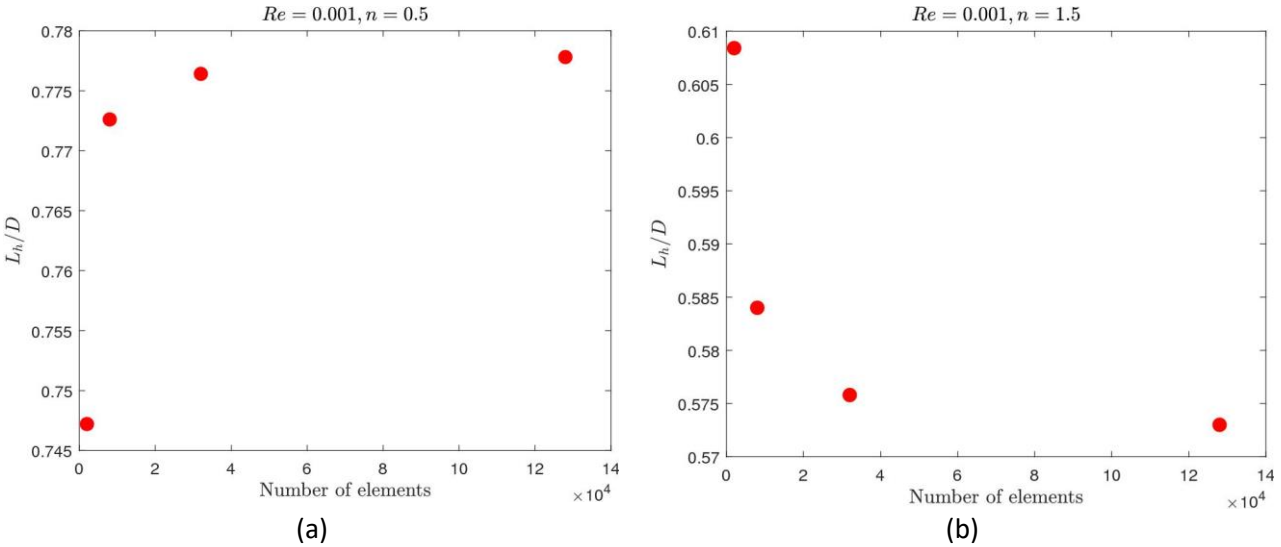

(a) (b)

Fig. 2. Grid independence test for flow through tube having superhydrophobic transverse grooves at $Re = 0.001$ for (a) $n = 0.5$ and (b) $n = 1.5$

3.1 Effect on Development of Velocity Profile

In Figure 3, the axial velocity distributions at various axial locations (i.e., z/D = 0, 0.025, 0.125, 0.225, 0.325, 0.425 and at fully-developed region) for different power-law fluids are shown. The axial locations examined (i.e., z/D = 0.025, 0.125, 0.225, 0.325 and 0.425) are located at the center of rib of the first until the fifth successive groove-rib period. As can be deduced from this figure, the flow develops from initially a uniform velocity distribution until the fluid flow attains a consistent parabolic profile at successive rib locations in the hydrodynamically fully-developed region.

At no-slip region, the fluid particles in the layer in contact with the surface of the tube come to a complete stop and this causes the adjacent layer of fluid particles to slow down. To maintain the mass flow rate through the tube, the velocity of the fluid at the centerline is thus larger. With the presence of superhydrophobic transverse grooves, the fluid flow alternately experiences both fluid slip over the liquid-gas interface and zero velocity along the solid-liquid interface. Comparing to the overall shape of the fully-developed velocity profiles, it can be clearly observed that the velocity profile is flatter for shear-thinning fluid ($n = 0.5$) and sharper for shear-thickening fluid ($n = 1.5$), as compared to that of Newtonian fluid ($n = 1$).

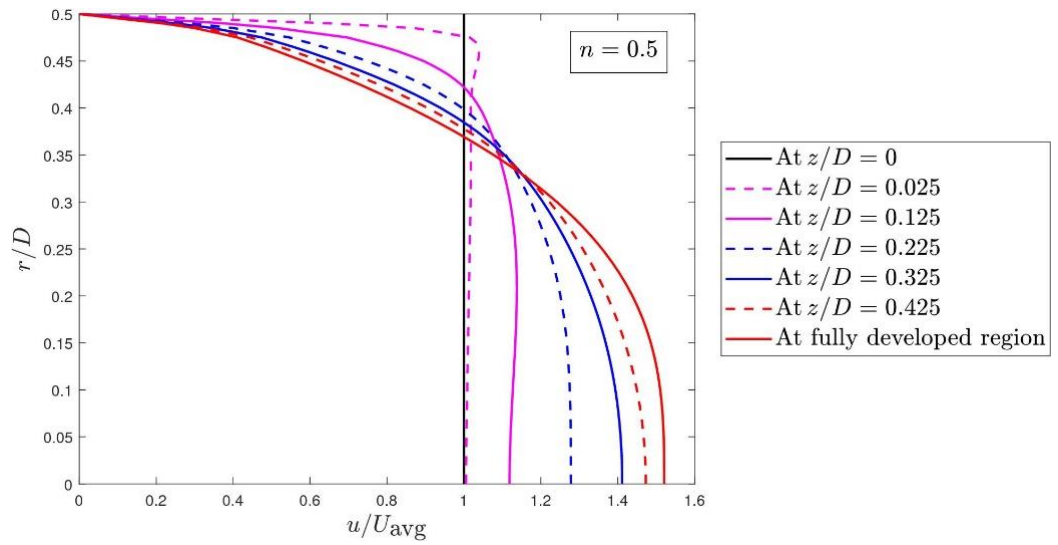

(a)

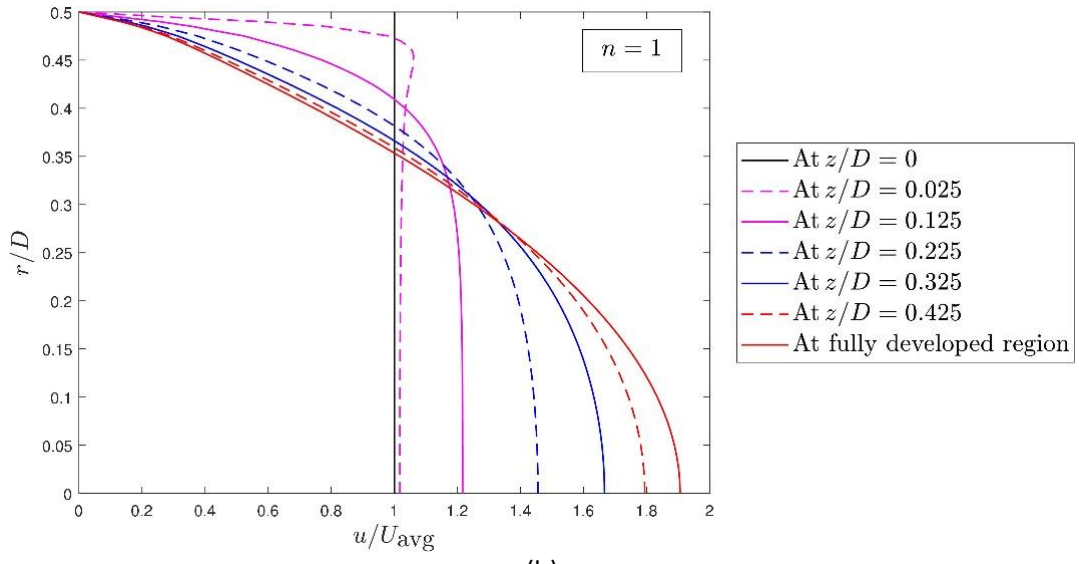

(b)

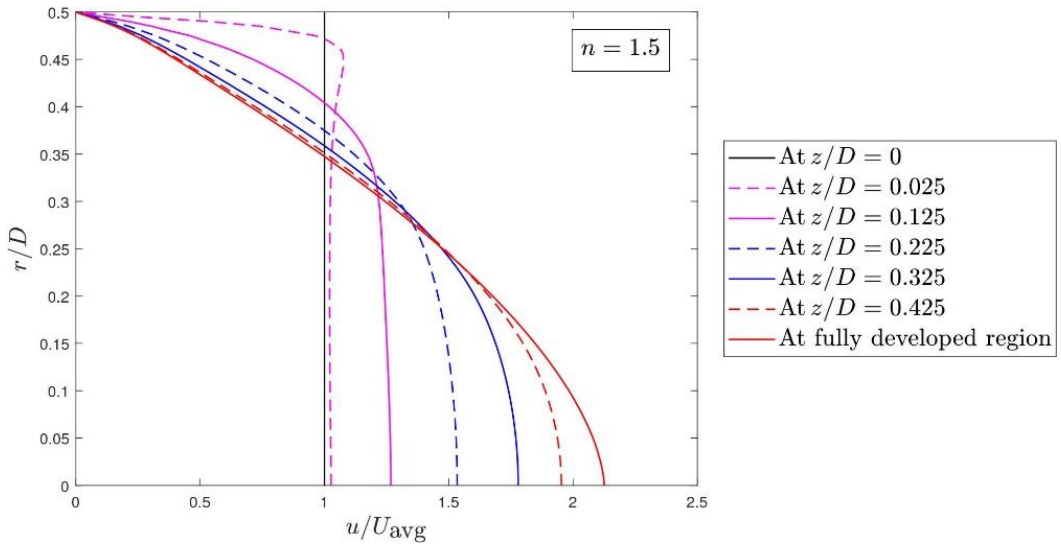

(c)

Fig. 3. Development of axial velocity along tube having superhydrophobic transverse grooves at $Re = 0.001$ for (a) $n = 0.5$, (b) $n = 1$, and (c) $n = 1.5$

In the vicinity of the wall where the shear rate is high, the apparent viscosity of shear-thinning fluid is lowered, thereby allowing higher velocity gradient in this region. On the other hand, the apparent viscosity is greater at the center of the tube. This allows smaller velocity gradient and thus giving rise to a flatter velocity profile at the center of the tube. In contrast, reverse behaviour of shear-thickening fluid exhibits a sharper shape of velocity profile at the tube center.

3.2 Effect on Centerline Velocity Distribution

It is also insightful to examine the influence of superhydrophobic transverse grooves on the centerline velocity distribution. As shown in Figure 4, the presence of these surface alters the centerline distribution where the magnitude of the axial velocity along the tube is relatively lower as compared to that of smooth walls. For superhydrophobic transverse grooves of $L = 0.1$ and $\delta = 0.5$, the maximum $u/U_{avg}$are approximately 1.5212, 1.9060 and 2.1258 for n = 0.5, 1 and 1.5, respectively. Comparatively, it would yield maximum u/U_{avg} value of 1.6651, 1.9988 and 2.2 for tube having smooth walls. The lower flow rate experienced in the center region of the flow is resulted from the redistribution of the flow with higher fluid flow allowed in the vicinity of the superhydrophobic wall. Despite the reduction on the maximum u/U_{avg}, non-Newtonian fluid with large power-law index (i.e., $n = 1.5$) still yields higher maximum u/U_{avg}value and vice versa, similar with that of smooth walls. It is also worth to highlight that the scale of superhydrophobic transverse grooves examined in this study is relatively small (i.e., L = 0.1 where the groove-rib periodic spacing is one-tenth of the tube diameter), thus the influence of these microstructures on the bulk flow is small. The alteration on the surface of the tube didn't change the shape of the velocity profile in the bulk region of the flow, as observed in Figure 4. This allows the velocity magnitude along the centerline to rise monotonically, similar to that of smooth walls.

3.3 Effect on Hydrodynamic Entrance Length

Variation of hydrodynamic entrance length with power-law index is plotted in Figure 5. For flows over superhydrophobic transverse grooves, numerical results show a decreasing entrance length

with the increase in the power-law index, *n*. This is similar with the trend exhibited by smooth wall. Comparatively, the entrance length for flow scenarios having superhydrophobic transverse grooves are constantly longer than that having smooth wall. For power-law fluid of $n = 0.5$ flowing over superhydrophobic transverse grooves of $L = 0.1$ and $\delta = 0.5$, the dimensionless entrance length (L_h/D) is predicted to be 0.7771, more than 3% increase than that of smooth wall. For shear-thickening fluid with power-law index of $n = 1.5$, L_h/D is estimated to be 0.5761.

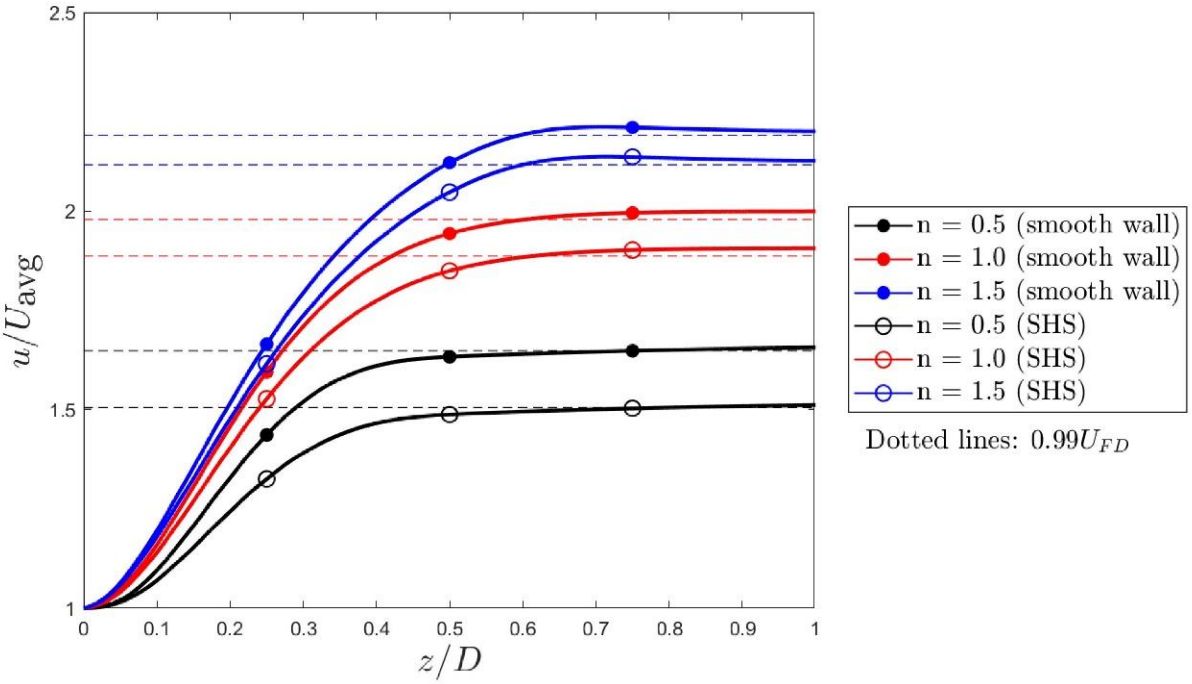

Fig. 4. Axial velocity profile for power-law fluids of different power-law indices along the centerline of tube having smooth wall, and superhydrophobic transverse grooves of $L = 0.1$ and $\delta = 0.5$ at $Re = 0.001$

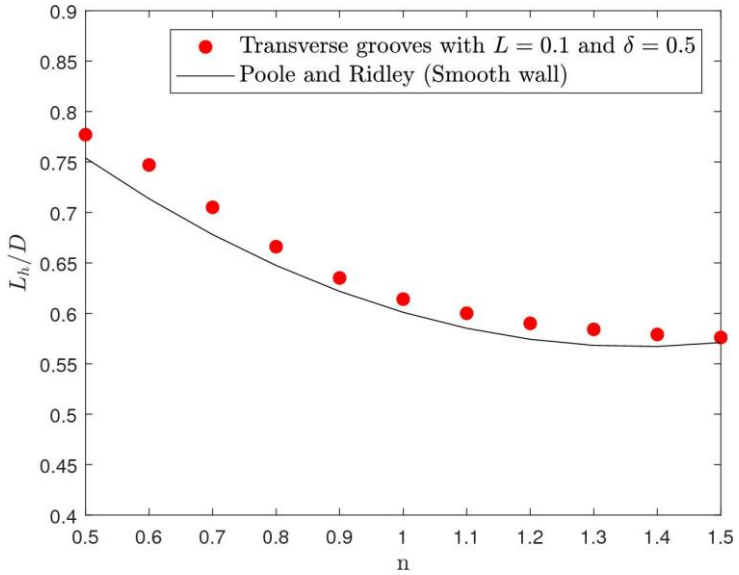

Fig. 5. Variation of entrance length with power-law index for flow having superhydrophobic transverse grooves. Solid black line denotes correlation data obtained from Eq. (1)

The entrance length variation with Reynold number in the range of $0.001 \leq Re \leq 1$ is plotted in Figure 6. As can be deduced from this figure, the dimensionless hydrodynamic entrance lengths are approximately constant at sufficiently low Reynolds numbers ($Re < 0.1$). This arises from the flow mechanism that is mainly governed by diffusion. At higher Reynold numbers $(Re > 0.1)$, the entrance length increases non-linearly with the increase in Reynolds number. Compared with that of smooth wall, the entrance length predicted for flow scenarios with superhydrophobic transverse grooves is consistently higher for both shear-thinning and shear-thickening fluids. At the same Reynolds number, the alteration on the tube surface by patterning superhydrophobic transverse grooves along the tube, gives rise to the creation and destruction of boundary layer when flow subsequently passing through rib and groove. With alternating groove-rib periodic pattern, this yields a continuous creation and destruction of boundary layers. The fluid accelerates and decelerates along the tube wall, and this could lead to the bulk of the fluid flow taking a longer length to become fully developed flow.

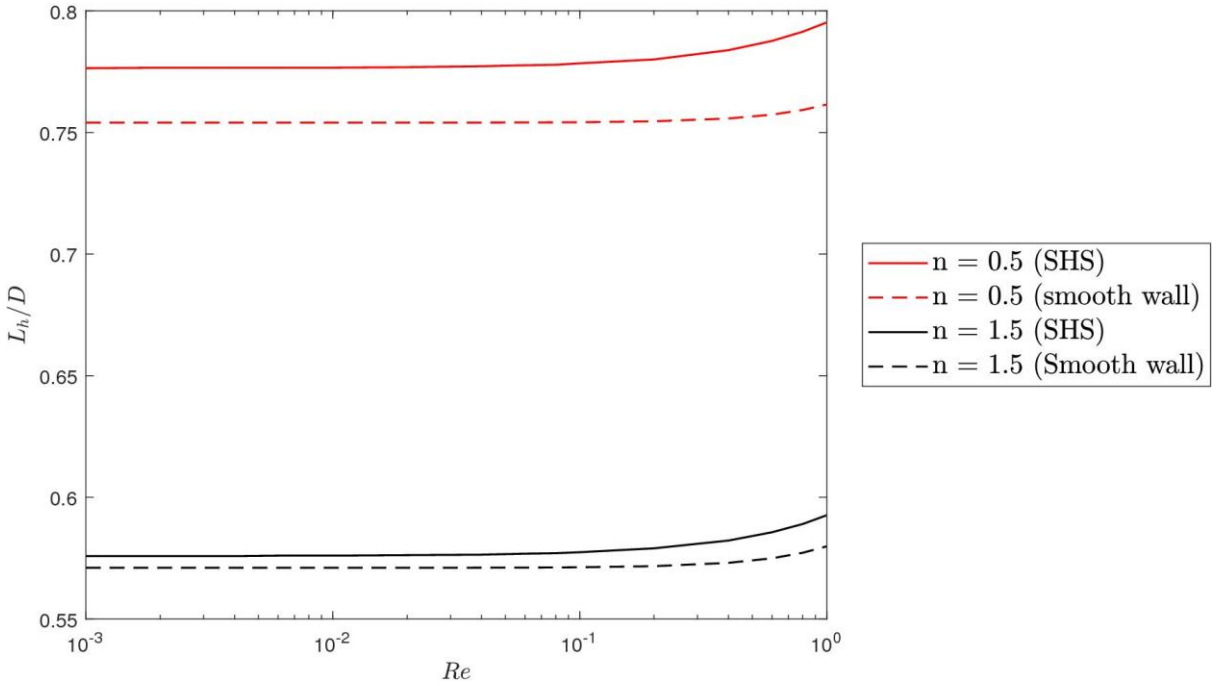

Fig. 6. Variation of entrance length with Reynolds number for flow scenarios in tubes having smooth wall and superhydrophobic transverse grooves

4. Conclusion

Numerical simulations were employed to investigate the developing flow of power-law fluids in pipe have superhydrophobic transverse grooves. The presence of these surfaces is found to exert influence on the flow velocity profile, velocity distribution along the centerline and the hydrodynamic entrance length. Examined for power-law index ranging from 0.5 to 1.5 at Reynolds number in the range $0.001 \leq Re \leq 1$, the hydrodynamic entrance length is predicted to be consistently longer than that of smooth wall. The numerical results shall hold when the hydrophobic effects remain throughout the tube and liquid didn't penetrate into the cavities in between microstructures along the tube surface.

Acknowledgement

The authors acknowledge Universiti Sains Malaysia Short-Term Grant No: 304/PMEKANIK/6315074 for the financial support.

References

[1] Cheng, Y. P., C. J. Teo, and B. C. Khoo. "Microchannel flows with superhydrophobic surfaces: effects of Reynolds number and pattern width to channel height ratio." *Physics of fluids* 21, no. 12 (2009): 122004.
[2] Ng, Chiu-On, and C. Y. Wang. "Effective slip for Stokes flow over a surface patterned with two-or three-dimensional protrusions." *Fluid Dynamics Research* 43, no. 6 (2011): 065504.
[3] Crowdy, Darren. "Frictional slip lengths for unidirectional superhydrophobic grooved surfaces." *Physics of Fluids* 23, no. 7 (2011): 072001.
[4] Davies, J., D. Maynes, B. W. Webb, and B. Woolford. "Laminar flow in a microchannel with superhydrophobic walls exhibiting transverse ribs." *Physics of fluids* 18, no. 8 (2006): 087110.
[5] Duan, Zhipeng, and Y. S. Muzychka. "Slip flow in the hydrodynamic entrance region of circular and noncircular microchannels." *Journal of Fluids Engineering* 132, no. 1 (2010): 011201.
[6] Durst, F., S. Ray, B. Ünsal, and O. A. Bayoumi. "The development lengths of laminar pipe and channel flows." *Journal of fluids engineering* 127, no. 6 (2005): 1154-1160.
[7] Fernandes, C., L. L. Ferrás, M. S. Araujo, and J. M. Nóbrega. "Development length in planar channel flows of inelastic non-Newtonian fluids." *Journal of Non-Newtonian Fluid Mechanics*255 (2018): 13-18.
[8] Ferrás, L. L., A. M. Afonso, M. A. Alves, J. M. Nóbrega, and F. T. Pinho. "Development length in planar channel flows of Newtonian fluids under the influence of wall slip." *Journal of Fluids Engineering* 134, no. 10 (2012): 104503.
[9] Haase, A. Sander, Jeffery A. Wood, Lisette MJ Sprakel, and Rob GH Lammertink. "Inelastic non-Newtonian flow over heterogeneously slippery surfaces." *Physical Review E* 95, no. 2 (2017): 023105.
[10] Lauga, Eric, and Howard A. Stone. "Effective slip in pressure-driven Stokes flow." *Journal of Fluid Mechanics* 489 (2003): 55-77.
[11] Metzner, A. B., and J. C. Reed. "Flow of non-newtonian fluids—correlation of the laminar, transition, and turbulent-flow regions." *Aiche journal* 1, no. 4 (1955): 434-440.
[12] Muzychka, Y. S., and R. Enright. "Numerical simulation and modeling of laminar developing flow in channels and tubes with slip." *Journal of Fluids Engineering* 135, no. 10 (2013): 101204.
[13] Ou, Jia, Blair Perot, and Jonathan P. Rothstein. "Laminar drag reduction in microchannels using ultrahydrophobic surfaces." *Physics of fluids* 16, no. 12 (2004): 4635-4643.
[14] Philippou, Maria, Zacharias Kountouriotis, and Georgios C. Georgiou. "Viscoplastic flow development in tubes and channels with wall slip." *Journal of non-newtonian fluid mechanics* 234 (2016): 69-81.
[15] Poole, R. J., and B. S. Ridley. "Development-length requirements for fully developed laminar pipe flow of inelastic non-Newtonian liquids." *Journal of Fluids Engineering* 129, no. 10 (2007): 1281-1287.
[16] Teo, C. J., and B. C. Khoo. "Analysis of Stokes flow in microchannels with superhydrophobic surfaces containing a periodic array of micro-grooves." *Microfluidics and nanofluidics* 7, no. 3 (2009): 353.
[17] Watanabe, Keizo, Yanuar Udagawa, and Hiroshi Udagawa. "Drag reduction of Newtonian fluid in a circular pipe with a highly water-repellent wall." *Journal of Fluid Mechanics* 381 (1999): 225-238.
[18] Yu, Kok Hwa, Yan Xu Tan, Mohd Sharizal Abdul Aziz, Yew Heng Teoh, and Mohd Zulkifly Abdullah. "The Developing Plane Channel Flow over Water-Repellent Surface Containing Transverse Grooves and Ribs." *Journal of Advanced Research in Fluid Mechanics and Thermal Sciences* 45, no. 1 (2018): 141-148.
[19] Yu, K. H., C. J. Teo, and B. C. Khoo. "Linear stability of pressure-driven flow over longitudinal superhydrophobic grooves." *Physics of Fluids* 28, no. 2 (2016): 022001.
[20] Yu, Kok Hwa, Yew Heng Teoh, Mohd Azmi Ismail, Chih Fang Lee, and Farzad Ismail. "Numerical Investigation on the Influence of Gas Area Fraction on Developing Flow in a Pipe Containing Superhydrophobic Transverse Grooves." *Journal of Advanced Research in Fluid Mechanics and Thermal Sciences* 45, no.1 (2018): 109-115.